Zeitschrift für Kristallographie 156, 305–321 (1981)

The effects of heating and dehydration on the crystal structure of hemimorphite up to 600 °C

B. J. Cooper, G. V. Gibbs,

Department of Geological Sciences

and F. K. Ross*

Department of Chemistry, Virginia Polytechnic Institute and State University, Blacksburg, Virginia 24061, USA

Received: January 6, 1981

Hemimorphite / Crystal structure / High temperature / Dehydration

Abstract. The crystal structure of hemimorphite, $Zn_4Si_2O_7(OH)_2 \cdot H_2O$, contracts upon dehydration caused by heating. X-ray intensity data were collected at 300 °C, at 600 °C and then at 22 °C. Anisotropic least-squares refinements of 532, 255, and 432 reflections in the space group *Imm*2, and $Z = 2$, resulted in unweighted *R*-factors of 0.046, 0.074, and 0.061, respectively. The following cell parameters were obtained during crystal alignment on the diffractometer:

	22 °C [1]	300 °C	600 °C	22 °C
a	8.367(5)	8.337(5)	8.268(5)	8.206(4)
b	10.730(6)	10.724(6)	10.784(8)	10.815(6)
c	5.115(3)	5.116(4)	5.113(3)	5.089(2)
V	459.2(4)	457.4(5)	455.9(5)	451.6(4)

The structure is a framework consisting of interconnected corrugated sheets composed of 3-membered rings of one SiO_4 and two $Zn(OH)O_3$ tetrahedra. Contraction of the structure above 300 °C is due to dehydration, and positive thermal expansion is observed in the dehydrated form. The structural mechanism of contraction is dependent upon the collapse of the cavities interconnected parallel to *c* towards the position of the expelled water molecule. The decrease in unit cell volume (ΔV_{uc}) is directly correlated with volume loss in the cavities (ΔV_c) and the increase in volume of the Zn tetrahedra (ΔV_z): $\Delta V_{uc} \sim 8\,\Delta V_z + 2\,\Delta V_c$. Zeolites with structural characteristics like hemimorphite show similar changes during molecular exchange reactions.

* Presently at: University of Missouri, Columbia, Missouri 65221

[1] After Hill et al. (1977)

Introduction

The effect of dehydration on the crystal structure of hemimorphite is of interest because the mineral has zeolitic characteristics. In studying the crystal structure at room temperature, Ito and West (1932), Barclay and Cox (1960), McDonald and Cruickshank (1967), Hill, Gibbs, Craig, Ross, and Williams (1977), and Takéuchi, Sasaki, Joswig, and Fuess (1978) demonstrated the presence of both hydroxyl groups and water molecules. Each hydroxyl group is strongly bonded to the structural framework, and hydrogen-bonded to water molecules located in a series of interconnected cavities (Hill et al., 1977; Takéuchi et al., 1978). Upon heating, water loss occurs in two stages, half the water content being lost in each stage (Zambonini, 1908; Faust, 1951; and Timofeeva, Tarnovskii, and Shafrinskii, 1967). The first stage is dehydration and only results in a structural readjustment in response to the loss of the water molecule (Roy and Mumpton, 1956; and Taylor, 1962). Dehydroxylation occurs next, causing a reconstructive transformation to β-Zn_2SiO_4 (Faust, 1951; Taylor, 1962; Götz and Masson, 1978).

The present X-ray diffraction study was undertaken to determine the effect of increasing temperature and molecular water loss on the crystal structure of hemimorphite and to attempt a rationalization of the mechanisms of dehydration based on the observed structural changes (Cooper, 1978).

Experimental

A transparent prismatic cleavage fragment ($0.23 \times 0.18 \times 0.18$ mm) was selected for this high temperature study from the same sample from Chihuahua, Mexico, from which Hill et al. (1977) obtained the crystal used in their room temperature neutron refinement of the structure. Single-crystal precession photographs of the fragment were found to be consistent with the space group *Imm*2. The fragment was mounted and heated using the procedure and heater described by Brown, Sueno, and Prewitt (1973) and Hochella (1977). The *a*-axis of the fragment was slightly inclined to the ϕ-axis of a Picker FACS-1 fully automated four-circle diffractometer.

The unit cell parameters were measured with Mo$K\alpha_1$ radiation ($\lambda = 0.70926$ Å) at $300° \pm 20°$C, $600° \pm 15°$C, and after heating (AH) to 600°C at $300° \pm 20°$C and $22° \pm 2°$C. These were then refined by least-squares methods to minimize the differences between calculated and observed angles 2θ, χ, and ω for 30 automatically centered reflections in the range $2\theta = 35-55°$ at 300°C and 22°C (AH), and $2\theta = 22°-44°$ at 600°C. The resulting cell dimensions and cell volumes are listed in Table 1.

X-ray intensity data for the structure analysis were collected at 300°, 600°, and 22°C (AH) to a maximum of $\sin\theta/\lambda = 0.7035$ using Nb-filtered Mo$K\alpha$ radiation ($\lambda = 0.71069$ Å) and a 2θ scan rate of 2° per minute. Backgrounds

Table 1. Cell edges (Å) and cell volume (Å^3) *vs* temperature

Temperature (°C)	*a*	*b*	*c*	*V*
22[a]	8.367(5)	10.730(6)	5.115(3)	459.2(4)
22	8.364(5)	10.724(6)	5.112(3)	458.5(4)
300[b]	8.342(5)	10.724(6)	5.117(4)	457.8(5)
300[c]	8.337(5)	10.724(6)	5.116(4)	457.4(5)
600[b]	8.279(6)	10.786(7)	5.114(3)	456.7(5)
600[c]	8.268(5)	10.784(8)	5.113(3)	455.9(5)
300[d]	8.237(5)	10.804(7)	5.106(3)	454.4(5)
22[d]	8.206(4)	10.815(6)	5.089(2)	451.6(4)
550[e]	8.25	10.75	5.10	452
600[f]	8.309	10.724	5.120	456.2

[a] After Hill et al. (1977), neutron refinement
[b] Before data collection
[c] After data collection
[d] After heating to 600°C
[e] After Taylor (1962), precession study on quenched sample
[f] Extrapolation, neglecting dehydration effect

Table 2. Refinement details

	300°C	600°C	22°C (AH)
Number of measurements	801	1279	2226
Maximum variation of reference reflections	±2.9%	±4.0%	±4.0%
Transmission factors			
Maximum:	0.32	0.32	0.32
Minimum:	0.12	0.13	0.13
Number of symmetry independent reflections	640	394	674
Number of reflections where $I < 2\sigma_I$	108	139	242
Number of reflections used in refinements	532	255	432
Isotropic refinement			
$R(F)$	0.085	0.093	0.066
$wR(F^2)$	0.101	0.065	0.052
Anisotropic refinement			
$R(F)$	0.046	0.074	0.061
wR(YO)	0.042	0.047	0.048
S	2.86	1.50	1.48
σ	2.31	1.80	1.76

were determined from 10-second stationary counts at both ends of the scan range of 2.4−2.63 2θ. Three standard reflections, remeasured after every 50 regular reflections in order to monitor crystal and instrument stability, showed no significant variation. The intensities were corrected for background, Lorentz, polarization, and absorption effects (based on actual crystal shape and μ values of 103.6 cm^{-1} at 300°C and 103.4 cm^{-1} after loss of the water molecule). The minimum and maximum transmission factors were 0.12 and 0.32, respectively. The low transmission factors were due to attenuation errors in the more intense peaks. Multiply measured and symmetry-equivalent reflections (consistent with point group *mm*2) were statistically weighted and averaged to yield a set of structure amplitudes, each with a standard deviation estimated from the equation $\sigma = [\sigma_I^2 + (0.02\,I)^2]^{0.5}/2\,I^{0.5}$, where I is the corrected raw intensity and σ_I is estimated from counting and averaging statistics. Of these data only those observations with $I > 2\,\sigma_I$ were included in the subsequent least-squares refinements. Table 2 lists pertinent information for the data reduction and refinements.

Refinement

The atomic coordinates of hemimorphite determined at room temperature by Hill et al. (1977) served as starting parameters for the 300°C structure refinement; the 300°C coordinates and the 600°C coordinates were used as the starting parameters for the 600°C refinement and the 22°C (AH) refinement, respectively. The unit cell origin was defined by fixing the z-coordinate of Zn at 0.0 (McDonald and Cruickshank, 1967). Scattering factors for Zn, Si, and O (neutral atoms) were obtained from International Tables for X-ray Crystallography (1974) and were corrected for both real and imaginary anomalous dispersion components. The three data sets were refined by least-squares minimization of the function $\Sigma\, w(|F_o| - |F_c|)^2$, where F_o and F_c are the observed and calculated structure amplitudes and $w = 1/\sigma^2$. Each refinement was first performed with isotropic temperature factors. Upon convergence of the isotropic refinement, difference syntheses showed anisotropy of the atoms and the loss of the water molecule above 300°C. Anisotropic refinement produced significantly better R-factors in all cases, except that it resulted in non-positive definite temperature factors for the 600°C and 22°C (AH) refinements. When the isotropic extinction coefficient (g) was added to the model the temperature factors remained non-positive definite and g varied insignificantly from zero. The non-positive definite temperature factors are due to the β_{23} term becoming negative for one of the oxygen atoms. The significance of this is uncertain since the value of β_{23} is less than one estimated standard deviation (*esd*) from zero. If the temperature factors are indeed non-positive definite, then the anisotropic model is not

accounting for a slight anharmonic motion of the atom. Conventional R values for each refinement are given in Table 2. A complete listing of calculated and observed structure amplitudes for each refinement is given in Table 3[2]. The final atomic and thermal parameters are listed in Table 4. Selected interatomic distances and angles are given in Table 5. Thermal corrections for interatomic distances have not been made because of uncertainty in selecting a model which adequately describes the effect of thermal motion on bond distances in hemimorphite. Programs utilized for

Table 4. Final fractional coordinates and thermal parameters for hemimorphite ($\times 10^4$)

Atom		22°C[a]	300°C	600°C	22°C (AH)
Zn	x	2047(1)	2043(1)	2074(2)	2091(2)
	y	1613(1)	1613(1)	1594(2)	1584(1)
	z	0	0	0	0
	β_{11}	29(1)	43(1)	87(3)	36(2)
	β_{22}	20(1)	23(1)	43(1)	15(1)
	β_{33}	66(4)	108(3)	168(6)	78(4)
	β_{12}	−5(1)	−10(1)	−15(2)	−9(2)
	β_{13}	−1(2)	18(4)	2(12)	6(8)
	β_{23}	3(2)	−2(4)	−15(11)	−12(8)
	B_{eq}[b]	0.81(2)	1.13(2)	2.05(4)	0.83(3)
Si	x	0	0	0	0
	y	1465(2)	1461(2)	1436(6)	1433(5)
	z	5076(5)	5092(14)	5199(33)	5193(23)
	β_{11}	23(2)	27(3)	62(7)	25(5)
	β_{22}	13(1)	9(2)	21(5)	12(4)
	β_{33}	45(6)	75(8)	104(27)	15(21)
	β_{12}	0	0	0	0
	β_{13}	0	0	0	0
	β_{23}	0(3)	−5(7)	8(18)	−17(12)
	B_{eq}	0.57(3)	0.65(5)	1.25(14)	0.46(11)
O(1)	x	1602(2)	1604(8)	1607(13)	1622(12)
	y	2055(1)	2054(6)	2047(13)	2062(10)
	z	6362(4)	6363(10)	6461(21)	6411(15)
	β_{11}	38(1)	47(11)	55(17)	47(16)
	β_{22}	26(1)	25(4)	39(10)	11(8)
	β_{33}	70(4)	119(16)	205(42)	94(29)
	β_{12}	−17(1)	−23(6)	−43(15)	−22(9)
	β_{13}	−9(2)	−16(10)	−76(30)	−66(18)
	β_{23}	9(2)	6(7)	−22(23)	−7(12)
	B_{eq}	1.00(2)	1.23(13)	1.82(26)	0.92(22)

[2] In Cooper (1978)

Table 4. (Continued)

Atom		22°C[a]	300°C	600°C	22°C (AH)
O(2)	x	0	0	0	0
	y	1669(2)	1684(8)	1662(19)	1600(19)
	z	1938(4)	1927(12)	2011(28)	1967(22)
	β_{11}	27(2)	32(13)	71(25)	82(24)
	β_{22}	33(1)	39(7)	62(18)	55(16)
	β_{33}	55(5)	64(21)	183(61)	62(43)
	β_{12}	0	0	0	0
	β_{13}	0	0	0	0
	β_{23}	4(2)	−6(11)	−80(32)	−20(27)
	B_{eq}	0.95(3)	1.12(18)	2.25(42)	1.81(36)
O(3)	x	3050(2)	3063(14)	3026(43)	3278(24)
	y	0	0	0	0
	z	410(6)	427(22)	557(48)	463(58)
	β_{11}	50(2)	58(14)	513(82)	171(41)
	β_{22}	18(1)	40(7)	53(19)	4(13)
	β_{33}	271(10)	304(65)	294(160)	490(158)
	β_{12}	0	0	0	0
	β_{13}	−30(4)	−43(22)	80(91)	160(70)
	β_{23}	0	0	0	0
	B_{eq}	1.69(4)	2.21(28)	6.52(98)	3.29(69)
O(4)	x	0	0	0	0
	y	0	0	0	0
	z	5912(6)	5897(22)	6067(47)	6038(35)
	β_{11}	54(3)	25(20)	189(168)	12(27)
	β_{22}	10(2)	7(8)	30(23)	2(19)
	β_{33}	124(9)	241(40)	285(106)	217(69)
	β_{12}	0	0	0	0
	β_{13}	0	0	0	0
	β_{23}	0	0	0	0
	B_{eq}	1.09(5)	1.18(26)	3.18(162)	0.89(45)
O(5)	x	5000	5000		
	y	0	0		
	z	5195(13)	5132(80)		
	β_{11}	164(10)	230(52)		
	β_{22}	277(12)	422(59)		
	β_{33}	221(19)	347(85)		
	β_{12}	0	0		
	β_{13}	0	0		
	β_{23}	0	0		
	B_{eq}	5.79(22)	9.82(100)		

[a] After Hill et al. (1977)

[b] $B_{eq} = \frac{4}{3}[\beta_{11} a^2 + \beta_{22} b^2 + \beta_{33} c^2]$ for the orthorhombic case

Table 5. Bond lengths, angles, and interatomic distances (Å)

	22°C[a]	300°C	600°C	22°C[b]
Tetrahedra:				
SiO_4				
Si–O(2)	1.620(3)	1.638(10)	1.648(22)	1.651(16)
–O(1) [2]	1.622(2)	1.618(7)	1.617(12)	1.618(10)
–O(4)	1.629(2)	1.621(5)	1.612(9)	1.609(8)
Mean	1.623(2)	1.624(4)	1.624(7)	1.624(6)
O(2)–Si–O(1) [2]	110.4(1)	109.9(3)	109.5(8)	109.6(6)
–O(4)	113.0(2)	113.2(6)	114.5(13)	111.8(10)
O(1)–Si–O(4) [2]	105.7(1)	106.2(4)	106.4(9)	107.6(8)
–O(1)	111.5(2)	111.5(5)	110.4(10)	110.7(8)
Mean	109.5(1)	109.5(2)	109.5(4)	109.5(3)
O(2)...O(1) [2]	2.662(2)	2.665(8)	2.667(15)	2.671(12)
O(4)	2.709(3)	2.720(11)	2.741(25)	2.699(20)
O(1)...O(4) [2]	2.591(2)	2.590(7)	2.585(12)	2.604(10)
O(1)	2.681(3)	2.675(14)	2.657(22)	2.662(20)
Mean	2.649(2)	2.651(4)	2.650(7)	2.652(6)
ZnO_4				
Zn–O(3)	1.935(2)	1.943(6)	1.912(15)	1.985(11)
–O(1)[c]	1.951(2)	1.950(6)	1.974(13)	1.937(8)
–O(1)[d]	1.956(2)	1.954(6)	1.914(11)	1.943(10)
–O(2)	1.980(2)	1.969(4)	2.001(8)	1.987(6)
Mean	1.956(1)	1.954(3)	1.950(6)	1.963(4)
O(3)–Zn–O(1)[c]	111.4(1)	111.0(4)	112.5(10)	109.9(6)
–O(1)[d]	113.7(1)	114.2(6)	117.0(8)	116.1(9)
–O(2)	110.4(1)	110.7(5)	108.0(12)	111.8(8)
O(1)[c]–Zn–O(1)[d]	105.82(7)	105.7(2)	106.3(4)	104.9(3)
–O(2)	107.47(9)	107.0(3)	104.6(5)	106.1(6)
O(1)[d]–Zn–O(2)	107.71(8)	107.8(3)	107.7(5)	107.5(9)
Mean	109.4(1)	109.4(2)	109.4(3)	109.4(3)
O(3)...O(1)[c]	3.211(2)	3.209(8)	3.232(14)	3.215(12)
O(1)[d]	3.259(3)	3.271(13)	3.261(23)	3.327(22)
O(2)	3.214(3)	3.219(12)	3.166(32)	3.288(21)
O(1)[c]...O(1)[d]	3.116(2)	3.113(8)	3.110(12)	3.074(11)
O(2)	3.169(2)	3.151(9)	3.144(15)	3.140(14)
O(1)[d]...O(2)	3.179(3)	3.169(8)	3.161(17)	3.165(13)
Mean	3.191(2)	3.189(4)	3.179(8)	3.202(7)

Table 5. (Continued)

	22°C[a]	300°C	600°C	22°C[b]
Si–O(4)–Si	149.5(2)	150.5(9)	148.0(20)	149.0(15)
Zn–O(1)–Zn	114.01(7)	114.2(3)	115.9(5)	116.2(4)
Zn–O(2)–Zn	119.8(1)	119.8(3)	118.0(7)	119.5(5)
Zn–O(3)–Zn	126.9(1)	126.2(6)	128.1(20)	119.4(10)
Zn–O(1)[c]–Si	116.7(1)	116.2(4)	116.0(8)	114.4(6)
Zn–O(1)[d]–Si	128.3(1)	128.5(4)	127.3(8)	128.5(6)
Zn–O(2)–Si [2]	119.47(6)	119.3(2)	120.2(4)	120.0(3)
Si...Si	3.144(4)	3.136(7)	3.098(13)	3.100(12)
Zn...Zn[e]	3.277(1)	3.278(3)	3.294(3)	3.294(2)
Zn...Zn[f]	3.425(2)	3.407(6)	3.429(5)	3.432(3)
Zn...Zn[g]	3.461(2)	3.464(5)	3.438(4)	3.426(3)
Zn...Zn[h]	4.932(2)	4.931(8)	4.855(4)	4.774(4)
Si...Zn[i]	3.050(4)	3.039(6)	2.999(14)	2.992(10)
Si...Zn[e]	3.219(2)	3.218(4)	3.221(5)	3.210(4)
Si...Zn	3.114(4)	3.117(6)	3.168(14)	3.155(10)
Zn–Si–Zn	100.3(1)	100.0(1)	97.4(2)	96.9(1)
O(3)...O(3)	3.263(3)	3.231(24)	3.264(71)	2.827(39)

[a] After Hill et al. (1977)
[b] After heating
[c] $\frac{1}{2}-x, \frac{1}{2}-y, z-\frac{1}{2}$
[d] $x, y, 1-z$
[e] $\frac{1}{2}-x, \frac{1}{2}-y, \frac{1}{2}$
[f] $-x, y, 0$
[g] $x, -y, 0$
[h] $1-x, y, 0$
[i] $x, y, 1$

solution, refinement and geometry calculations were local modifications of DATALIB, DATASORT, OR XFLS3, OR FFE3, FOURIER, and ORTEP2. These programs are included in the World List of Crystallographic Computer Programs (3rd ed. and supplements). Polyhedral volumes were calculated using the program POLYVOL (Swanson and Peterson, 1980).

Discussion

Structure and dehydration

The structure of hemimorphite was first described by Ito and West (1932) and later confirmed by Barclay and Cox (1960), McDonald and Cruickshank

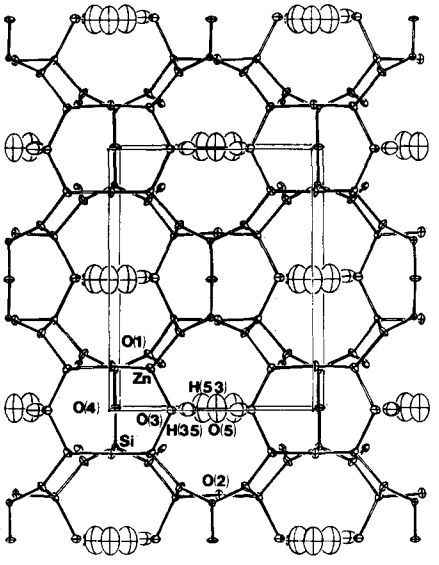

Fig. 1. ORTEP drawing of the hemimorphite structure viewed up *c*. A single unit cell has been outlined in the drawing. Thermal ellipsoids for all atoms represent 50% probability surfaces. Plotted using data of Hill et al. (1977)

(1967), Hill et al. (1977), and Takéuchi et al. (1978), the latter two papers being the first to describe the location of the hydrogen atoms in detail. According to Zoltai (1960), hemimorphite shoult be classified as a framework silicate because its SiO_4 and $Zn(OH)O_3$ tetrahedra share corners throughout the structure. The framework consists of corrugated layers parallel to (010) composed of 3-membered rings of one SiO_4 and two $Zn(OH)O_3$ tetrahedra (Fig. 1). The layers, joined at the O(3) (hydroxyl oxygen) and O(4) atoms, form 4-, 6-, and 8-membered rings parallel to (001) with $Zn_4(OH)_2O_{10}$, $Zn_4Si_2(OH)_2O_{16}$, and $Zn_4Si_4(OH)_4O_{20}$ composition, respectively (Fig. 2). The cavities formed between 6-membered rings are interconnected to form channelways along the *c*-axis (Fig. 3). At room temperature the water molecule [represented by O(5)] is oriented parallel to (010) in the center of the cavities, and is hydrogen-bonded to the hydroxyl groups (Hill et al., 1977; Takéuchi et al., 1978). Upon heating, the water molecule is expelled from the structure between 393° and 657° C (Faust, 1951). Hill et al. (1977) suggested that the water molecule is expelled through the 6-membered rings by a process of proton exchange with the hydroxyl groups.

Cell parameters

The unit cell parameters of hemimorphite listed in Table 1 vary linearly upon cooling from 600° C (Figs. 4 and 5). The dashed lines in the figures represent

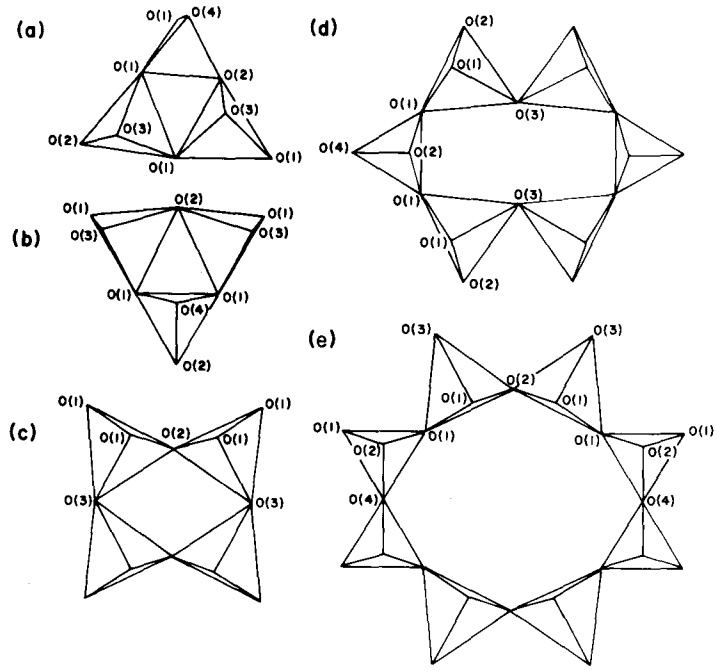

Fig. 2. Ring formations found in the crystal structure of hemimorphite. **a** 3-Membered ring viewed down [110]. **b** Other 3-membered ring viewed down [010]. **c** 4-Membered ring viewed down [001]. **d** 6-Membered ring viewed down [001]. **e** 8-Membered ring viewed down [001]. All tetrahedra in this figure point up, out of the page

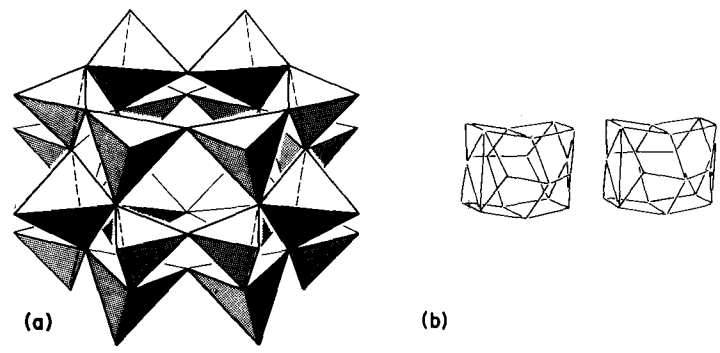

Fig. 3. Cavity containing the water molecule viewed down [101]. **a** Tetrahedral drawing, dashed lines indicating back edge of tetrahedra. **b** Polyhedral drawing

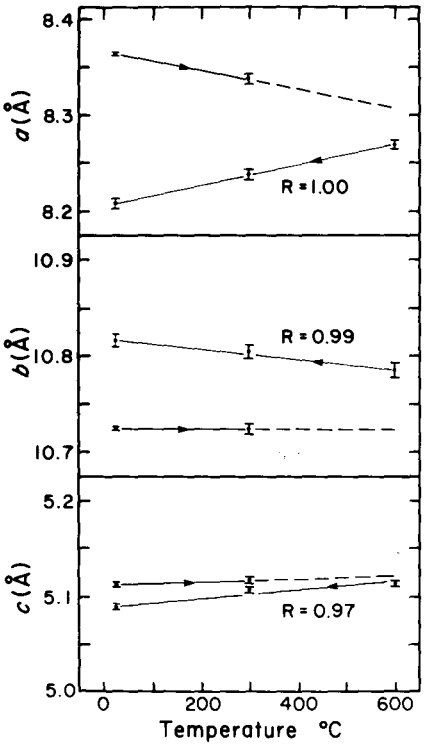

Fig. 4
Variation of *a*, *b*, and *c* unit cell parameters with increasing temperature for hemimorphite. Error bars represent ± one standard deviation. Arrows indicate direction of heating, then cooling

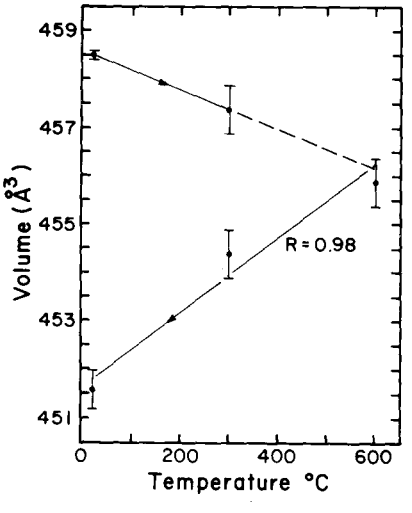

Fig. 5
Variation of unit cell volume with increasing temperature for hemimorphite. Error bars represent ± one standard deviation. Arrows indicate direction of heating, then cooling

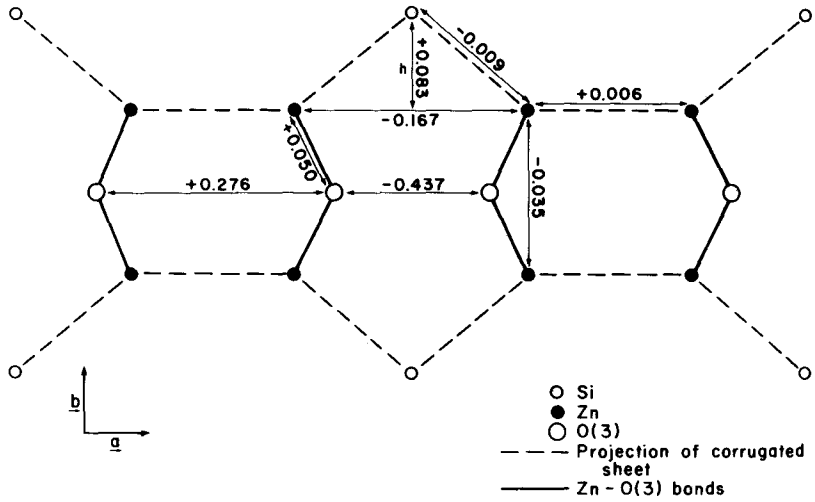

Fig. 6. Corrugated sheets viewed down [001], showing interconnecting Zn–O(3) bonds. Numbers indicate changes in interatomic distances (Å) after dehydration and heating. Negative values imply contraction, and positive values imply expansion and h is the height of the Zn–Si–Zn triangle

the expected trend if linear thermal expansion (or contraction) was maintained upon heating to 600°C. Heating to 300°C causes a decrease of the *a* cell edge, while *b* and *c* remain unchanged. Continued heating causes dehydration, resulting in a 0.07 Å contraction along *a* and a 0.06 Å expansion along *b*. Cooling from 600°C to 22°C causes further shortening of *a*, lengthening of *b*, and contraction of *c*. These results can be explained in terms of the effects of heating and dehydration on the hydroxyl positions and corrugated sheets.

The O(3)...O(3) separation decreases by 0.44 Å parallel to [100] and 0.02 Å parallel to [001] after dehydration, implying that O(3)...O(5) and H...H repulsions within the cavity had kept the framework expanded. Takéuchi (personal communication, 1979) has suggested the formation of hydrogen bonds between the hydroxyl groups. This bonding and the adjacent O(3)...O(3) and H...H repulsions would account for the present O(3)...O(3) separation and concomitant Zn–O(3)–Zn angle decrease of 7.5°. Corresponding to this angular decrease is a Zn...Zn separation decrease and a lengthening of Zn–O(3) by 0.05 Å. The observed contraction of *a* corresponds to the reduction of O(3)...O(3) and Zn...Zn distances parallel to [100]. The expansion of *b* cannot be accounted for in terms of interatomic distances actually parallel to [010], but must be rationalized in terms of positional changes and their effect on the corrugated sheet (Fig. 6). The mean interatomic distances within the sheet remain relatively unchanged with dehydration, which results in a 0.01 Å decrease in the Si... Zn distance.

Therefore, as Zn... Zn decreases, the Zn – Si – Zn angle must decrease, and h increases. The difference between the increase in h and the Zn... Zn distance decreases along [010] corresponds to the observed expansion of b. Despite this expansion, the unit cell volume shows a decrease after dehydration and cooling because the Zn... Zn distance parallel to [100] decreases about twice as fast as h increases, and the Zn... Zn and O(3)... O(3) distances parallel to [001] also decrease.

Polyhedra

The variation of polyhedral volumes with temperature is given in Table 6 and shown in Figure 7. The changes in the dimensions of the silicate tetrahedron are insignificant over the temperature interval studied, whereas the dimensions of the zincate tetrahedron show a significant increase at room temperature after dehydration. The increased volume of the zincate tetrahedron is directly related to the lengthening of the Zn – O(3) bond length, with the other Zn – O bond lengths remaining unchanged within error. As expected, the large cavity containing the water molecule shrinks significantly following the expulsion of the water from the structure. This can be rationalized by the same means used to explain the net decrease of the unit cell volume. In fact, the unit cell volume decrease may be expressed as approximately $8\,\Delta V_z + 2\,\Delta V_c$, where ΔV_z and ΔV_c are the volume changes of the zincate tetrahedron and the cavity, respectively.

Table 6. Polyhedral volumes (Å^3) *vs* temperature

	Temperature (°C)	Volume (Å^3)
Zincate tetrahedra	22	3.83
	300	3.81
	600	3.77
	22 (AH)	3.85
Silicate tetrahedra	22	2.19
	300	2.19
	600	2.19
	22 (AH)	2.20
Cavities	22	161.79
	300	160.94
	600	161.18
	22 (AH)	157.88

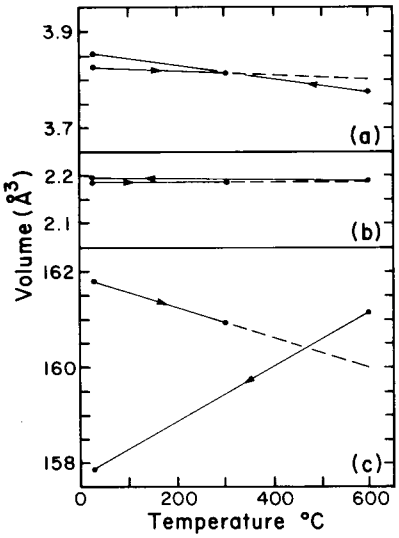

Fig. 7
Variation of polyhedral volumes with increasing temperature for hemimorphite.
a Zincate tetrahedra.
b Silicate tetrahedra.
c Cavity. Arrows indicate direction of heating, then cooling

Isotropic equivalent temperature factors

Isotropic equivalent temperature factors (B_{eq}) for Zn, Si, and the oxygen atoms are given in Table 4 and shown in Figure 8. The discontinuity between 300° and 600°C may again be ascribed to dehydration.

Although both Zn and Si are tetrahedrally coordinated, the initial B_{eq} and the rate of increase of B_{eq} are higher for Zn than for Si. This is to be expected because the Zn–O bond strengths are less than the Si–O bond strengths, since $d(\text{Zn}-\text{O}) > d(\text{Si}-\text{O})$ and $q_{\text{Zn}} < q_{\text{Si}}$. Therefore, Zn has more freedom of movement than Si. The oxygen atom B_{eq}'s do not change significantly until dehydration of the structure. The 3-coordinated oxygens [O(1) and O(2)] show lower rates of increase of B_{eq} after dehydration than the 2-coordinated bridging oxygens [O(3) and O(4)] which have a large component of thermal vibration parallel to the *c*-axis. The molecular water oxygen atom [O(5)] B_{eq} increases rapidly from 22°C to 300°C because O(5) is only hydrogen-bonded to the hydroxyl groups. The O(3) and O(2) atoms have higher room temperature B_{eq}'s after heating, which implies that the water molecule placed some constraint on their thermal motion. For the hydroxyl oxygen [O(3)] this is understandable because it was originally constrained by hydrogen bonds to the water molecule. The increase in B_{eq} for O(2) is more difficult to explain, but probably arises from a longer Si–O(2) bond length which allows increased motion into the cavity along the *x* and *y* directions. The O(2) atom also has the only non-positive definite anisotropic temperature factor which may either be due to anharmonic motion of either the O(2) atom or possibly

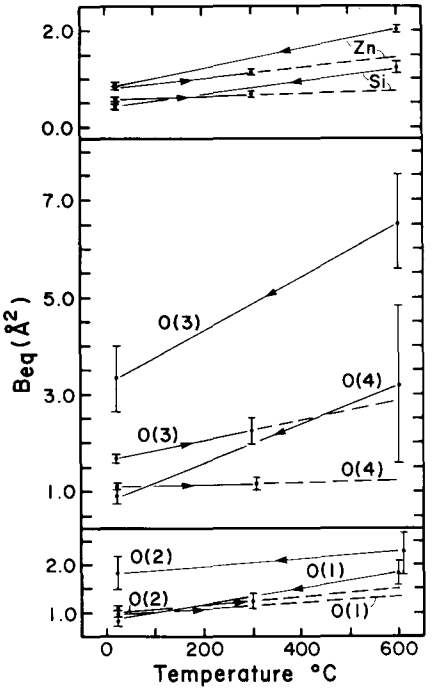

Fig. 8
Variation with increasing temperature of the equivalent isotropic temperature factors. Error bars represent ± one standard deviation. Arrows indicate direction of heating, then cooling

the Si atom, or it may be due to errors in the data. Further evidence of anharmonic thermal motion of the Si atom has been given by Takéuchi et al. (1978).

Comparison of hemimorphite to zeolites

Hemimorphite and zeolites are hydrous tetrahedral framework silicates having large interconnected cavities. Like some X and Y type zeolites, hemimorphite contains framework hydroxyl groups. Hemimorphite is not a zeolite because hemimorphite has Zn rather than Al in tetrahedral coordination, and the Si/Zn ratio is 0.5, whereas in zeolites the Si/Al ratio is usually greater than one. Moreover, exchangable cations have not yet been observed in hemimorphite. Finally, the hydrated free aperture of hemimorphite is a narrow rectangle 0.56×6.32 Å (dehydrated free aperture $= 0.13 \times 6.35$ Å), while the smallest zeolite free aperture dimension is 2.2 Å, assuming a radius for oxygen of 1.35 Å (Breck, 1974).

Despite the differences in structure and composition, and especially the small free aperture, the hemimorphite framework responds to dehydration like a zeolite. Most zeolites and hemimorphite may be dehydrated without a

major structural change, and differential thermal analysis curves show low temperature endotherms and continuous dehydration over a broad temperature range indicating a reversible dehydration (Faust, 1951; Breck, 1974; Götz and Masson, 1978). It is assumed therefore, that rehydration would occur under conditions of T and P_{H_2O} that would force water molecules into the cavities. This has been shown to occur in zeolites, but not to our knowledge for hemimorphite. Hemimorphite and zeolites containing structural hydroxyl groups both undergo reconstructive transformation upon loss of the hydroxyl water.

The dehydration of hemimorphite without structural destruction, even with the narrow free aperture, implies that either the aperture is very flexible at higher temperatures or that only the oxygen atom passes through the 6-member ring by a process of proton exchange with the hydroxyl groups as suggested by Hill et al. (1977). In any case, the small free aperture rules out the use of hemimorphite as a molecular sieve, which many zeolites are used for. Hemimorphite could possibly serve as a "sieve" on an atomic or ionic scale.

Acknowledgements. The authors wish to express their gratitude to the Earth Science Section of the National Science Foundation for supporting this study with grant EAR77-23114 and the Research Division at VPI & SU for defraying the computer costs. We wish to thank Dr. Y. Takéuchi, Dr. R. J. Hill, Dr. F. D. Bloss, and Dr. P. H. Ribbe for their constructive criticisms and helpful suggestions. Special thanks to Dr. J. B. Higgins for getting the data reduction programs started, Mrs. Ramonda Haycocks for typing parts of the manuscript, and Mrs. Sharon Chiang for drafting most of the figures.

References

Barclay, G. A., Cox, E. G.: The structure of hemimorphite. Z. Kristallogr. **113**, 23–29 (1960)

Breck, D. W.: Zeolite Molecular Sieves, 771 pp. New York: John Wiley & Sons 1974

Brown, G. E., Sueno, S., Prewitt, C. T.: A new single-crystal heater for the precession camera and four-circle diffractometer. Amer. Mineral. **58**, 698–704 (1973)

Cooper, B. J.: The effects of heating and dehydration on the crystal structure of hemimorphite up to 600° C. M. S. Thesis, Virginia Polytechnic Institute and State University, Blacksburg, Virginia 1978

Faust, G. T.: Thermal analysis and X-ray studies of sauconite and of some zinc minerals of the same paragenetic association. Amer. Mineral. **36**, 795–822 (1951)

Götz, J., Masson, C. R.: Trimethylsilyl derivatives for the study of silicate structure. Part 4. The conversion of hemimorphite into willemite. J. Chem. Soc. Dalton, 1134–1138 (1978)

Hill, R. J., Gibbs, G. V., Craig, J. R., Ross, F. K., Williams, J. M.: A neutron diffraction study of hemimorphite. Z. Kristallgr. **146**, 241–259 (1977)

Hochella, M. F., Jr.: High temperature crystal chemistry of hydrous Mg- and Fe-rich cordierites. M.S. Thesis, Virginia Polytechnic Institute and State University, Blacksburg, Virginia 1977

International Tables for Crystallography, Vol. IV, Kynock, Birmingham, England, p. 99 and 149, 1974

Ito, T., West, J.: The structure of hemimorphite ($H_2Zn_2SiO_5$). Z. Kristallogr. **83**, 1–8 (1932)

McDonald, W. W., Cruickshank, D. J. W.: Refinement of the structure of hemimorphite. Z. Kristallogr. **124**, 180–191 (1967)

Roy, D. M., Mumpton, F. A.: Stability of minerals in the system $ZnO-SiO_2-H_2O$. Econ. Geol. **51**, 432–443 (1956)

Swanson, D. K., Peterson, R. C.: Polyhedral volume calculations. Can. Mineral. **18**, 153–156 (1980)

Takéuchi, Y., Sasaki, S., Joswig, W., Fuess, H.: X-ray and neutron diffraction study of hemimorphite. Proc. Japan Acad. **54**, 577–582 (1978)

Taylor, H. F. W.: The dehydration of hemimorphite. Amer. Mineral. **47**, 932–944 (1962)

Timofeeva, Z. F., Tarnovskii, G. N., Shafrinskii, Y. S.: Products of the thermal decomposition of calamine. Rentgenogr. Miner. Syr'ya **6**, 91–94 (1967). (Russ.) (not seen; extracted from Chem. Abstracts, **70**, # 7204, 1969)

Zambonini, F.: Contributo allo studio dei silicati idrati. Atti dell Real Accad. dell Scienze fis. e math. Napoli, [2] **14**, No. 1 (1908)

Zoltai, T.: Classification of silicates and other minerals with tetrahedral structures. Amer. Mineral. **45**, 960–973 (1960)